



Article

# Cytotoxic Furanoditerpenes from the Sponge *Spongia tubulifera* Collected in the Mexican Caribbean

Dawrin Pech-Puch <sup>1</sup>, Jaime Rodríguez <sup>1,\*</sup> , Bastien Cautain <sup>2</sup>,  
Carlos Alfredo Sandoval-Castro <sup>3</sup>  and Carlos Jiménez <sup>1,\*</sup> 

<sup>1</sup> Centro de Investigaciones Científicas Avanzadas (CICA) e Departamento de Química, Facultade de Ciencias, Universidade da Coruña, 15071 A Coruña, Spain

<sup>2</sup> Fundación MEDINA, Centro de Excelencia en Investigación de Medicamentos Innovadores en Andalucía, Avda. del Conocimiento 34, 18016 Granada, Spain

<sup>3</sup> Universidad Autónoma de Yucatán, Campus de Ciencias Biológicas y Agropecuarias, Facultad de Medicina Veterinaria y Zootecnia, Km. 15.5 Carretera Mérida-Xmatkuil, Apdo. Postal 4-116, Itzimná Mérida, Yucatán, Mexico

\* Correspondence: [jaime.rodriguez@udc.es](mailto:jaime.rodriguez@udc.es) (J.R.); [carlos.jimenez@udc.es](mailto:carlos.jimenez@udc.es) (C.J.)

Received: 4 July 2019; Accepted: 12 July 2019; Published: 16 July 2019



**Abstract:** Two new spongian furanoditerpenes, 3 $\beta$ -hydroxyspongia-13(16),14-dien-2-one (**1**) and 19-dehydroxy-spongian diterpene 17 (**2**), along with five known terpenes, the spongian furanoditerpenes 9-nor-3-hydroxyspongia-3,13(16),14-trien-2-one (**3**), 3 $\beta$ ,19 dihydroxyspongia-13(16),14-dien-2-one (epispongiadiol) (**4**) and spongian diterpene 17 (**5**), the furanoditerpene ambliol C (**6**), and the sesterterpene scalarin (**7**), were isolated from the methanolic extract of the sponge *Spongia tubulifera*, collected in the Mexican Caribbean. The planar structures of the new compounds were elucidated by 1D/2D NMR and IR spectroscopic analysis, high resolution electrospray mass spectrometry (HRESIMS), and comparison of their spectral data with those reported in the literature. Absolute configurations were determined by comparison of the experimental electronic circular dichroism (ECD) spectrum with those calculated by time-dependent density functional theory (TDDFT). Compounds **1**, **4**, and **6** displayed weak cytotoxic activity against different human tumour cell lines.

**Keywords:** spongian furanoditerpenes; marine sponge; *Spongia tubulifera*; ECD-TDDFT; cytotoxicity

## 1. Introduction

Specimens belonging to the genus *Spongia* have been subjected to numerous chemical investigations yielding a wide variety of C21 and other linear furanoterpenes, spongian diterpenes, scalarane sesterterpenoids, sesquiterpene quinones, sterols (including secosterols), and macrolides [1], many of which have shown biological activities including antibacterial [2,3], antiviral [4], antitumoral [5,6], and anti-inflammatory functions [7].

In our continuing investigations of diterpenes from marine organisms [8,9], and in particular from marine sponges [10], we have focused our attention on the sponge *Spongia tubulifera*, collected in the Mexican Caribbean, because of the cytotoxic activity found in its methanolic extract. To the best of our knowledge, the only previous reports of *S. tubulifera* were a comparative study of the fatty acids composition of specimens of this sponge collected at Ahogado Reef near La Parguera, Puerto Rico [11] and the assays of the antimicrobial activity against *Staphylococcus aureus* and *Candida albicans* of the organic extracts of specimens collected at Urabá Gulf reefs in the Colombian Caribbean [12].

In this paper, we elucidate the structures of two new spongian furanoditerpenes, 3 $\beta$ -hydroxyspongia-13(16),14-dien-2-one (**1**) and 19-dehydroxyspongian diterpene 17 (**2**), along with

five known terpenes, 3–7, and we evaluate their cytotoxic activity against a panel of five human tumour cell lines.

## 2. Results and Discussion

Specimens of the sponge *S. tubulifera*, collected by hand and scuba diving off the coast of the Mexican Caribbean, were extracted several times with CH<sub>3</sub>OH/CH<sub>2</sub>Cl<sub>2</sub> to give an extract which showed cytotoxic activity. The organic extract was subsequently partitioned between H<sub>2</sub>O/CH<sub>2</sub>Cl<sub>2</sub>, and the CH<sub>2</sub>Cl<sub>2</sub> portion was further fractionated into hexane, CH<sub>2</sub>Cl<sub>2</sub>, and aqueous methanolic fractions. The hexane fraction was submitted to silica gel flash chromatography using a gradient mixture of hexane and EtOAc to yield enriched terpene fractions that were then submitted repeatedly to reversed-phase HPLC separation (H<sub>2</sub>O/CH<sub>3</sub>OH mixtures) to yield 1–3 and 6. The CH<sub>2</sub>Cl<sub>2</sub> fraction was fractionated by solid phase extraction (SPE) with a RP-18 column using a stepped gradient from H<sub>2</sub>O, CH<sub>3</sub>OH, and CH<sub>2</sub>Cl<sub>2</sub> to yield enriched terpene fractions that were separated by RP-HPLC using H<sub>2</sub>O/CH<sub>3</sub>OH mixtures to afford 4, 5, and 7 (Figure 1).

Compound 1 was obtained as a colorless white powder. The molecular formula of 1 was determined on the basis of the M<sup>+</sup> peak at *m/z* 316.2014, observed in its HREIM spectrum (calculated for C<sub>20</sub>H<sub>28</sub>O<sub>3</sub>, 316.2038, 7 degrees of unsaturation) and from its <sup>13</sup>C NMR spectrum. Its IR spectrum displayed signals at 3500 and 1745 cm<sup>-1</sup>, suggesting the presence of a hydroxyl group and a ketone carbonyl functionality, respectively.

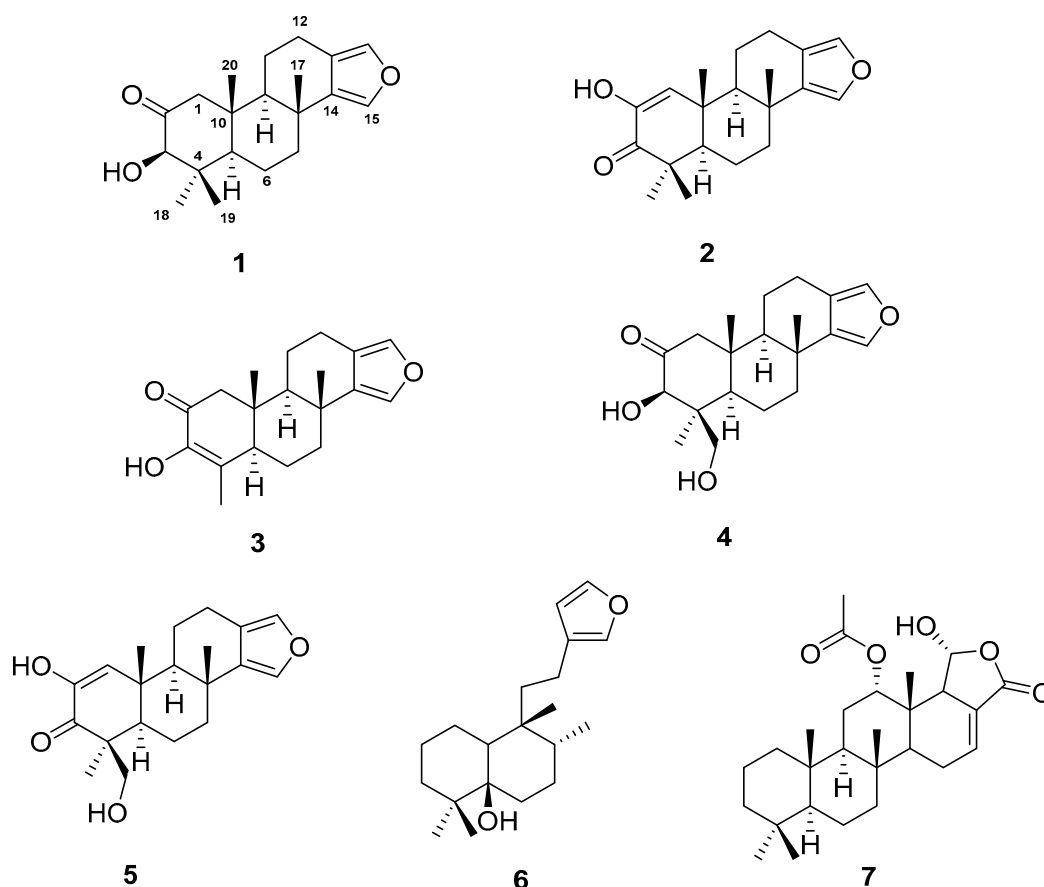
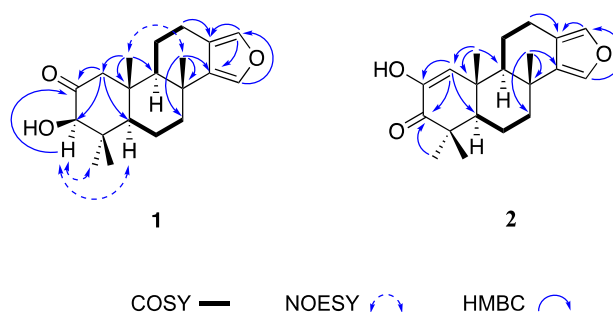


Figure 1. Structures of 1–7 isolated from *Spongia tubulifera*.

The <sup>13</sup>C NMR spectrum of 1 shows 20 signals (Table 1, Supplementary Material, Table S1) that, in combination with the <sup>1</sup>H NMR and HSQC spectra, indicated the presence of a spongian furanditerpene bearing four tertiary methyl groups ( $\delta_{\text{H}}/\delta_{\text{C}}$  1.23, *s*/26.0; 1.21, *s*/29.4; 0.73, *s*/16.5; and 0.88, *s*/17.3), a 3,4-disubstituted furan ring ( $\delta_{\text{H}}/\delta_{\text{C}}$  7.12, *s*/135.3; 7.07, *s*/137.1; 119.4; and 136.8),

one ketone carbonyl group ( $\delta_C$  211.1), a hydroxyl group at  $\delta_H$  3.48, and an oxymethine  $sp^3$  carbon ( $\delta_H/\delta_C$  3.90, d/ 83.1). Comparison of the NMR data of **1** with those of reported for other spongian furanoditerpenes, along with the HMBC correlations shown in Figure 2, indicated that **1** has a similar structure to 3 $\alpha$ -hydroxyspongia-13(16),14-dien-2-one isolated from an unidentified *Spongia* collected in Australia [13]. The differences of the proton and carbon chemical shifts at C-3, e.g.,  $\delta_H/\delta_C$  3.90 (d,  $J = 1.5$  Hz)/ 83.1 in **1** instead of  $\delta_H/\delta_C$  4.36 (d,  $J = 1.5$  Hz)/ 80.1 in 3 $\alpha$ -hydroxyspongia-13(16),14-dien-2-one, suggested that they differed only in the stereochemistry at C-3, and thus, **1** must be its 3 $\beta$  isomer. The NOESY correlations from H-3 at  $\delta_H$  3.90 to H-5 at  $\delta_H$  1.62 and H-18 at  $\delta_H$  1.21 indicated that these protons were in the same face of the molecule, confirming the  $\beta$ -orientation of the hydroxyl group at C-3. The relative configuration of the remaining stereogenic centers in **1** was also confirmed by its NOESY correlations (Figure 2). These data indicated that **1** is a new spongian furanoditerpene derivative with a 3 $\beta$ -hydroxyspongia-13(16),14-dien-2-one structure.



**Figure 2.** Key  $^1H$ - $^1H$  COSY, NOESY, and HMBC correlations of **1** and **2**.

The absolute configurations of the stereogenic carbons of **1** were determined by comparison of the experimental and simulated electronic circular dichroism (ECD) spectra generated by time-dependent density functional theory (TDDFT) calculations. Overall, the two possible enantiomers for **1**, (3*R*,5*R*,8*R*,9*R*,10*R*)-**1** and (3*S*,5*S*,8*S*,9*S*,10*S*)-**1**, were initially submitted to a conformational search with the Maestro Suite (Schrödinger). Four conformers were found within a 10.0 kcal/mol energy threshold from global minimum. All these conformers were geometrically optimized by a density functional theory (DFT) method at the HSEH1PBE/cc-pVDZ functions (see computational details in the experimental section). The resulting ECD spectra were combined by Boltzmann weighting to give a composite spectrum for each enantiomer. Comparison of the experimental and calculated ECD spectra for **1** showed excellent agreement with the (3*R*,5*R*,8*R*,9*R*,10*R*)-**1** enantiomer (Figure 3). Thus, the absolute configurations of C-3, C-5, C-8, C-9, and C-10 were determined as 3*R*, 5*R*, 8*R*, 9*R*, and 10*R*, respectively.

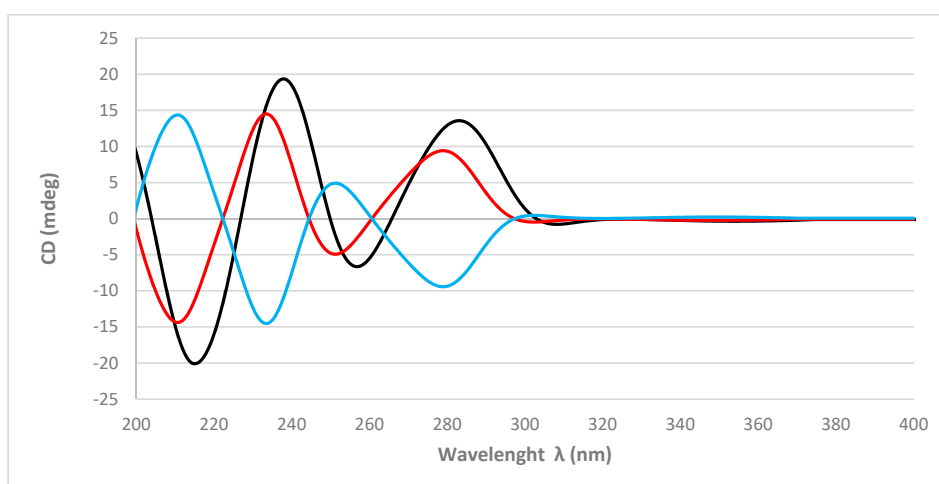


**Figure 3.** Experimental electronic circular dichroism (ECD) spectrum (black line) of **1** and calculated ECD spectrum (red line) for (3*R*,5*R*,8*R*,9*R*,10*R*)-**1** and (blue line) for (3*S*,5*S*,8*S*,9*S*,10*S*)-**1**.

**Table 1.**  $^{13}\text{C}$  (125 MHz) and  $^1\text{H}$  (500 MHz) NMR Data in  $\text{CDCl}_3$  of **1** and **2**.

Position	1		2	
	$\delta_{\text{C}}$ , type	$\delta_{\text{H}}$ , mult. (J in Hz)	$\delta_{\text{C}}$ mult.	$\delta_{\text{H}}$ , mult. (J in Hz)
1	53.3, CH	2.67, d (12.1) 2.13, d (12.1)	128.3, CH	6.54, s
2	211.1, C		144.3, C	
3	83.1, CH	3.90, d (1.5)	201.2, C	
4	45.7, C		44.3, C	
5	55.0, C	1.62, m	54.5, C	1.80, m
6	18.6, $\text{CH}_2$	1.66, m 1.80, m	19.1, $\text{CH}_2$	1.67, m
7	40.7, $\text{CH}_2$	1.68, m 2.20, m	40.4, $\text{CH}_2$	1.66, m 2.18, m
8	34.7, C		34.9, C	
9	56.1, CH	1.50, m	51.7, CH	1.48, dd (11.8, 1.7)
10	43.8, C		38.8, C	
11	18.9, $\text{CH}_2$	1.67, m	18.8, $\text{CH}_2$	1.91, dt (7.0, 1.7)
12	20.7, $\text{CH}_2$	2.49, m 2.82, m	20.7, $\text{CH}_2$	2.51, dddd (16.2, 12.2, 7.0, 1.7) 2.83, ddt (16.2, 6.3, 1.5)
13	119.4, C		119.5, C	
14	136.8, C		137.3, C	
15	135.3, CH	7.12, s	135.0, CH	7.09, s
16	137.1, CH	7.07, s	137.2, CH	7.06, s
17	26.0, $\text{CH}_3$	1.23, s	26.7, $\text{CH}_3$	1.28, s
18	29.4, $\text{CH}_3$	1.21, s	20.6, $\text{CH}_3$	1.16, s
19	16.5, $\text{CH}_3$	0.73, s	27.3, $\text{CH}_3$	1.23, s
20	17.3, $\text{CH}_3$	0.88, s	21.7, $\text{CH}_3$	1.22, s
OH		3.48, d (1.5)		5.93, s

The molecular formula of **2**, isolated as a colorless white powder, was established as  $\text{C}_{20}\text{H}_{26}\text{O}_3$  based on the  $[\text{M} + \text{Na}]^+$  at  $m/z$  337.1803 in its (+)-HRESIM spectrum (calculated for  $\text{C}_{20}\text{H}_{26}\text{O}_3\text{Na}$ , 337.1780, 8 degrees of unsaturation) and on NMR data (Table 1, Supplementary Material, Table S2). The IR spectrum of **2** shows absorptions from the hydroxyl ( $3505\text{ cm}^{-1}$ ) and a conjugated ketone carbonyl ( $1650\text{ cm}^{-1}$ ) groups.

The 20 carbon signals observed in the  $^{13}\text{C}$  NMR spectrum of **2** along with the presence of two  $\alpha$ -furan proton signals ( $\delta_{\text{H}}$  7.09 and 7.06) and four tertiary methyl groups ( $\delta_{\text{H}}$  1.28, 1.23, 1.22, and 1.16)

in its  $^1\text{H}$  NMR spectrum were indicative of a spongian furanoditerpene structure. The planar structure of **2** was established by a combination of 1D and 2D NMR spectroscopy. Comparison of the NMR data of **2** with those of **1** (see Table 1) revealed that they shared the same framework at the B, C, and D rings but differed in the A-ring. Signals in the  $^{13}\text{C}$  NMR spectrum of **2** for the conjugated ketone carbonyl group at  $\delta_{\text{C}}$  201.2 (C-3) and two  $sp^2$  carbons, the non-protonated carbon at  $\delta_{\text{C}}$  144.3 (C-2) and the methine carbon at  $\delta_{\text{C}}$  128.3 (C-1), were consistent with the presence of a conjugated  $\alpha,\beta$ -unsaturated ketone moiety.

The key  $^1\text{H}$ - $^{13}\text{C}$  long range correlations between the olefinic proton at  $\delta_{\text{H}}$  6.54 (H-1) and the olefinic carbon at  $\delta_{\text{C}}$  144.3 (C-2), the ketone carbonyl carbon at  $\delta_{\text{C}}$  201.2 (C-3) and the carbon at  $\delta_{\text{C}}$  54.5 (C-5), along with the HMBC correlation from the methyl singlet at  $\delta_{\text{H}}$  1.22 (H-20) to the olefinic carbon at  $\delta_{\text{C}}$  128.3 (C-1) placed the  $\alpha,\beta$ -unsaturated ketone in the A-ring (Figure 2). The exchangeable proton signal at  $\delta_{\text{H}}$  5.93 was indicative of an enolized  $\alpha$ -diketone moiety in the A-ring. The NMR data for this part of the molecule (see Table 1) are in agreement with those observed for other diterpenes containing the same A-ring in the tetracyclic framework such as spongian diterpene **17** (**5**), previously reported from the nudibranch *Doriprismatica* (= *Glossodoris*) *atromarginata* [14]. The diagnostic HMBC correlations displayed by the  $\alpha$ -furan proton signals and the methyl groups Me-17 and Me-18 displayed in Figure 2 confirm **2** as a new spongian furanoditerpene that was named 19-dehydroxy-spongian diterpene **17**.

As in **1**, the absolute configurations of the stereogenic carbons of **2** were determined by comparison of the experimental to those generated by TDDFT on the two possible enantiomers. The two possible enantiomers for **2**, (5*R*,8*R*,9*R*,10*R*)-**2** and (5*S*,8*S*,9*S*,10*S*)-**2**, were initially submitted to a conformation search with the Maestro Suite (Schrödinger). Thus, 4 conformers were found within a 10.0 Kcal/mol energy threshold from a global minimum. All these conformers were geometrically optimized by density functional theory method at the HSEH1PBE/cc-pVDZ function (see computational details in experimental section). As shown in Figure 4, the calculated ECD spectra for the (5*R*,8*R*,9*R*,10*R*)-**2** and its experimental data were almost identical. Thus, the absolute configurations of C-5, C-8, C-9, and C-10 of **2** were determined as 5*R*, 8*R*, 9*R*, and 10*R*, respectively.

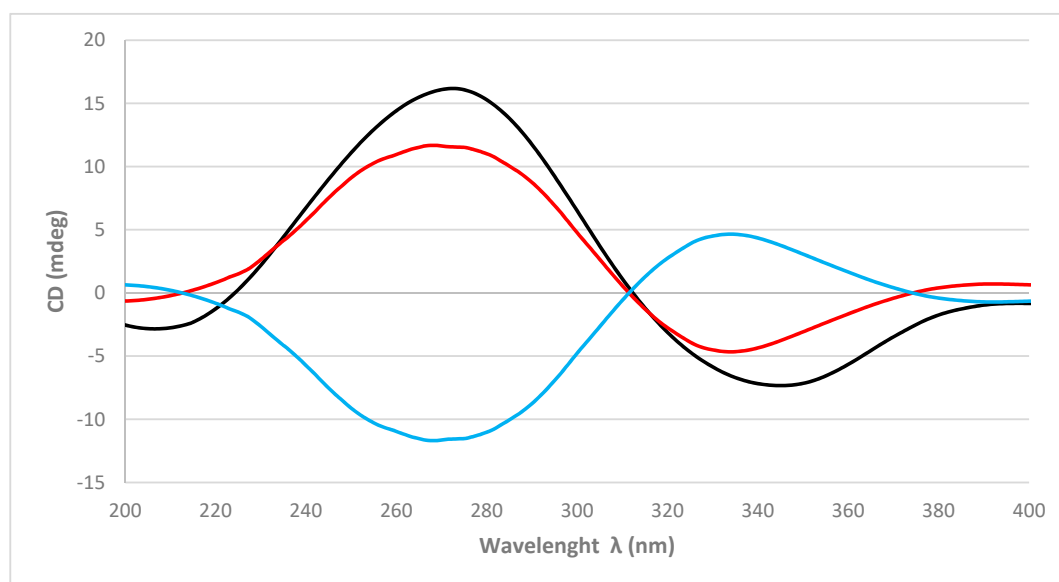


**Figure 4.** Experimental ECD spectrum (black line) of **2** and calculated ECD spectrum (red line) for (5*R*,8*R*,9*R*,10*R*)-**2** and (blue line) for (5*S*,8*S*,9*S*,10*S*)-**2**.

Spectral data ( $^1\text{H}$  and  $^{13}\text{C}$  NMR, MS,  $[\alpha]_{\text{D}}^{25}$ ) of **3** and **4** were identical with those reported for 19-*nor*-3-hydroxyspongia-3,13(16),14-trien-2-one (epispongiadiol) [15] and 3 $\beta$ -19-dihydroxyspongia-13(16),14-dien-2-one [16], respectively, isolated from an unidentified *Spongia*; while the NMR/spectroscopic data for **5** matched with those reported for spongian diterpene **17**, isolated from the nudibranch

*Doriprismatica* (= *Glossodoris atromarginata* [14]; the NMR/spectroscopic data for **6** were identical with those reported for ambiol C, isolated from the sponge *Dysidea amblia* [17], and the NMR/spectroscopic data for **7** matched with those reported for scalarin from the sponge *Cacospongia scalaris* by Fattorusso et al. [18] and later on from *Spongia nitens* by Cimino et al. [19].

The isolated compounds were submitted to biological activity assays. MTT ((3-(4,5-Dimethylthiazol-2-yl)-2,5-diphenyltetrazolium bromide)) assays were performed on human lung carcinoma A549 ATCC®CCL-185TM, human skin melanoma A2058 ATCC®CRL-11147TM, hepatocyte carcinoma HepG2 ATCC®HB-8065TM, breast adenocarcinoma MCF7 ATCC®HTB-22TM, and pancreas carcinoma MiaPaca-2 ATCC®CRL-1420TM with doxorubicin as a positive control [20]. Compounds **1** and **4** showed a weak cytotoxic activity, while **6** exhibited the highest cytotoxic activity with IC<sub>50</sub> values from 28.3 to 11.7 µM (Table 2). Previous biological studies of **4** indicated cytotoxic activity against the human tumor cell lines A549 (human lung carcinoma cells), HT-29 (human colorectal carcinoma cells), and P388 (leukemia cells lines) [21] and antiviral activity against VSV (vesicular stomatitis virus) and HSV-1 (herpes simplex virus type 1) [4]. On the other hand, it was reported that **6** induced *Artemia* sp. to death in a test of settlement and metamorphosis inhibition of larvae or juveniles [22]. Additionally, **1–7** did not show any significant antibacterial activity against *Acinetobacter baumannii*, *Pseudomonas aeruginosa*, *Klebsiella pneumoniae*, *Staphylococcus aureus*, or antiviral activity against human adenoviruses (HAdV5 and HAdV5-GFP).

**Table 2.** Cytotoxic Activity Data (IC<sub>50</sub> in µM) of **1**, **4**, and **6**<sup>a</sup>.

Tumour Cell Lines	Compound			
	<b>1</b>	<b>4</b>	<b>6</b>	Doxorubicin
A549 (lung)	88.1 ± 7.9	73.7 ± 6.3	28.3 ± 2.1	0.4 ± 0.2
A2058 (skin)	71.4 ± 2.5	53.9 ± 0.6	22.9 ± 0.7	0.1 ± 0.1
HepG2 (hepatocyte)	91.3 ± 15.8	60.1 ± 5.0	24.3 ± 0.2	0.1 ± 0.1
MCF-7 (breast)	nd	nd	19.9 ± 3.3	5.1 ± 0.5
MiaPaca-2 (pancreas)	90.0 ± 44.8	nd	11.7 ± 0.9	6.6 ± 0.5

<sup>a</sup> IC<sub>50</sub>, compound concentration that produces 50% inhibition on cell growth as compared to control cells. nd: not detected.

### 3. Materials and Methods

#### 3.1. General Experimental Procedures

Optical rotations were measured on a JASCO DIP-1000 polarimeter, with a Na (589 nm) lamp and filter. IR spectra were measured on a FTIR Bruker Vector 22 spectrometer. <sup>1</sup>H, <sup>13</sup>C, and 2D NMR spectra were recorded on a Bruker Avance 500 spectrometer at 500 and 125 MHz, respectively, using CDCl<sub>3</sub>. Low resolution electrospray mass spectrometry (LRESIMS) and high resolution electrospray mass spectrometry (HRESIMS) experiments were performed on the Applied Biosystems QSTAR Elite system. LREIMS and HREIMS were performed on the Mass Spectrometer Thermo MAT95XP. HPLC separations were performed on the Agilent 1100 liquid chromatography system equipped with a solvent degasser, quaternary pump, and diode array detector (Agilent Technologies, Waldbronn, Germany) using a semipreparative reversed phase column Luna C18, 5 µ, 100 Å, 250 × 10 mm. Precoated silica gel plates (Merck, Kieselgel 60 F254, 0.25 mm) were used for TLC analysis, and the spots were visualized under a UV light (254 nm) or by heating the plate pretreated with H<sub>2</sub>SO<sub>4</sub>/H<sub>2</sub>O/AcOH (1:4:20).

#### 3.2. Animal Material

The sponge *Spongia tubulifera* was collected by hand and traditional scuba diving off the coast of the Mexican Caribbean (18°48'22.17"N / 87°39'32.61"W) at depths ranging from 10 to 15 m in March 2017. Samples were frozen immediately after collection. A voucher specimen 17YUE11ST was deposited in the Phylum Porifera Gerardo Green National Collection of the Instituto de Ciencias del

Mar y Limnología (ICMyL) at the National Autonomous University of México (UNAM) in Ciudad de Mexico.

### 3.3. Extraction and Isolation

Sliced bodies of *S. tubulifera* (wet weight, 157.7 g; dry weight, 40.2 g) were exhaustively extracted with CH<sub>3</sub>OH-CH<sub>2</sub>Cl<sub>2</sub> (1:1, 3 × 1.5 L) at 25 °C for 24 h each extraction. The combined extracts were concentrated under reduced pressure to give 12.0 g of a crude residue that was first partitioned between CH<sub>2</sub>Cl<sub>2</sub>/H<sub>2</sub>O (1:1 *v/v*). The resulting aqueous portion was extracted with n-butanol (200 mL) to yield the n-butanol fraction (1.44 g). The organic phase was concentrated under reduced pressure and partitioned between 10% aqueous CH<sub>3</sub>OH (400 mL) and hexane (2 × 400 mL) to give, after removing the solvent under reduced pressure, 526 mg of the hexane fraction. The H<sub>2</sub>O content (% *v/v*) of the methanolic fraction was adjusted to 50% aqueous CH<sub>3</sub>OH, and the mixture was extracted with CH<sub>2</sub>Cl<sub>2</sub> (100 mL) to afford, after removing the solvent under reduced pressure, 1.51 g of the CH<sub>2</sub>Cl<sub>2</sub> fraction and 2.38 g of the remaining aqueous methanolic fraction. The hexane fraction (526 mg) was subjected to a flash chromatography column on silica gel using a stepped gradient from hexane to EtOAc to give 14 fractions (FHC1-C14). Separation of the fraction FHC2, eluted with hexane/EtOAc (9:1, 93.9 mg), by RP-HPLC with a mobile phase consisting of an isocratic at 100% CH<sub>3</sub>OH at a flow rate of 2.0 mL/min afforded **6** (13.5 mg; *t<sub>R</sub>* = 8.4 min). Separation of the fraction FHC3, eluted with hexane/EtOAc (9:1, 20.0 mg), by RP-HPLC (isocratic 100% CH<sub>3</sub>OH, flow rate 2.0 mL/min) gave **2** (2.6 mg; *t<sub>R</sub>* = 9.7 min) and **6** (2.6 mg; *t<sub>R</sub>* = 8.9 min). Separation of the fraction FHC4, eluted with hexane/EtOAc (8:2, 9.0 mg), by RP-HPLC with a mobile phase consisting of 5 min gradient from 90% to 95% of CH<sub>3</sub>OH in H<sub>2</sub>O, followed by a 10 min isocratic at 95% of CH<sub>3</sub>OH in H<sub>2</sub>O and, finally, a 5 min gradient from 95% to 100% of CH<sub>3</sub>OH in H<sub>2</sub>O at a flow rate of 2.0 mL/min yielded **2** (2.0 mg; *t<sub>R</sub>* = 12.6 min). Separation of the fraction FHC5, eluted with hexane/EtOAc (8:2, 21.0 mg), by RP-HPLC with a mobile phase consisting of 5 min gradient from 90% to 95% of CH<sub>3</sub>OH in H<sub>2</sub>O, followed by a 15 min isocratic at 95% of CH<sub>3</sub>OH in H<sub>2</sub>O and, finally, a 10 min gradient from 95% to 100% of CH<sub>3</sub>OH in H<sub>2</sub>O at a flow rate of 2.0 mL/min afforded **2** (1.7 mg; *t<sub>R</sub>* = 13.0 min) and **3** (1.5 mg; *t<sub>R</sub>* = 12.0 min). Separation of the fraction FHC7, eluted with hexane/EtOAc (8:2, 27.2 mg), by RP-HPLC (isocratic 100% CH<sub>3</sub>OH, flow rate 2.0 mL/min) yielded **1** (3.0 mg; *t<sub>R</sub>* = 16.8 min). Separation of the fraction FHC8, eluted with hexane/EtOAc (8:2, 20.9 mg), by RP-HPLC with a mobile phase consisting of 5 min gradient from 90% to 95% of CH<sub>3</sub>OH in H<sub>2</sub>O followed by a 15 min isocratic at 95% of CH<sub>3</sub>OH in H<sub>2</sub>O and, finally, a 1 min gradient from 95% to 100% of CH<sub>3</sub>OH in H<sub>2</sub>O at a flow rate of 2.0 mL/min afforded **1** (1.8 mg; *t<sub>R</sub>* = 11.0 min). The dichloromethane fraction (1.51 g) was subjected to solid phase extraction (SPE) with RP-18 column (Merck KGaA) using a stepped gradient from H<sub>2</sub>O to CH<sub>3</sub>OH and then CH<sub>2</sub>Cl<sub>2</sub>, to give 6 fractions: H<sub>2</sub>O (100%), H<sub>2</sub>O/CH<sub>3</sub>OH (2:1, 1:1, and 1:2), CH<sub>3</sub>OH (100%), and CH<sub>2</sub>Cl<sub>2</sub> 100%. The fraction eluted with H<sub>2</sub>O/CH<sub>3</sub>OH (1:2) was submitted to RP-HPLC separation using a mobile phase consisting of 20 min gradient from 50% to 100% of CH<sub>3</sub>OH in H<sub>2</sub>O followed by a 10 min isocratic at 100% of CH<sub>3</sub>OH at a flow rate of 2.0 mL/min to afford **4** (9.2 mg; *t<sub>R</sub>* = 10.0 min). Separation of the fraction eluted with CH<sub>3</sub>OH (100%) by RP-HPLC using a mobile phase consisting of 30 min gradient from 80% to 100% of CH<sub>3</sub>OH in H<sub>2</sub>O at a flow rate of 2.0 mL/min afforded **7** (5.0 mg; *t<sub>R</sub>* = 26.7 min) and **5** (3.1 mg; *t<sub>R</sub>* = 29.7 min).

### 3.4. Computational Calculations

Conformational searches were performed by using the corresponding module implemented in the Maestro Quantum mechanical software. An OPLS 2005 force field with chloroform as the solvent was used, and torsional enhanced sampling with 1000 or 10,000 steps was fixed using an energy window of 10 kcal/mol. Molecular geometry optimizations were performed at the DFT theoretical level using the Gaussian 09W package firstly with a B3LYP/6-31G(d) combination and then with HSEH1PBE/cc-pVDZ auto for energy and frequency calculations. After removing redundant conformers, theoretical Boltzmann energy population-weighted ECD was calculated by using two

combinations: PBEPBE/6-311++(3d,2p) or CAM-B3LYP/6-311++(3d,2p), both with 24 states. Graphical theoretical ECD curves were obtained using the open software SpecDis V.1.71 (Berlin, Germany, 2017, <https://specdis-software.jimdo.com>) [23].

### 3.5. Metabolite Characterization

**(3R, 5R, 8R, 9R, 10R) 3 $\beta$ -Hydroxyspongia-13(16),14-dien-2-one (1):** Colorless white powder;  $[\alpha]_D^{25} - 10.5$  (c 0.1, CHCl<sub>3</sub>); IR (ATR neat)  $\nu_{\max}$  3500, 2920, 2810, 1745, 1430, 1371, 1229, 1120, 1050, 1038, 955, 882 cm<sup>-1</sup>; <sup>1</sup>H NMR (500 MHz) and <sup>13</sup>C NMR (125 MHz) see Table 1; HREIMS  $m/z$  316.2014 [M]<sup>+</sup> (calcd. for C<sub>20</sub>H<sub>28</sub>O<sub>3</sub>, 316.2038).

**(5R, 8R, 9R, 10R) 19-Dehydroxy-spongian diterpene 17 (2):** Colorless white powder;  $[\alpha]_D^{25} + 18.7$  (c 0.1, CHCl<sub>3</sub>); IR (ATR neat)  $\nu_{\max}$  3505, 2950, 2855, 2325, 1650, 1430, 1370, 1230, 1120, 1050, 1038, 955, 880, cm<sup>-1</sup>; <sup>1</sup>H NMR (500 MHz) and <sup>13</sup>C NMR (125 MHz) see Table 1; (+)-HRESIMS  $m/z$  337.1803 [M + Na]<sup>+</sup> (calcd. for C<sub>20</sub>H<sub>26</sub>O<sub>3</sub>Na, 337.1780).

**19-nor-3-Hydroxyspongia-3,13(16),14-trien-2-one (3):** Colorless white powder;  $[\alpha]_D^{25} + 2.7$  (c 0.1, CHCl<sub>3</sub>); (+)-HREIMS  $m/z$  300.1719 [M]<sup>+</sup> (calcd. for C<sub>19</sub>H<sub>24</sub>O<sub>3</sub>, 300.1725).

**3 $\beta$ , 19-Dihydroxyspongia-13(16),14-dien-2-one (epispongiadiol) (4):** Yellow powder;  $[\alpha]_D^{25} + 18.2$  (c 0.1, CHCl<sub>3</sub>); (+)-HRESIMS  $m/z$  355.1890 [M + Na]<sup>+</sup> (calcd. for C<sub>20</sub>H<sub>28</sub>O<sub>4</sub>Na, 355.1885).

**Spongian diterpene 17 (5):** Yellow powder;  $[\alpha]_D^{25} - 20.4$  (c 0.1, CHCl<sub>3</sub>); (+)-HRESIMS  $m/z$  353.1723 [M + Na]<sup>+</sup> (calcd. for C<sub>20</sub>H<sub>26</sub>O<sub>4</sub>Na, 353.1723).

**Ambliol C (6)** Yellow powder;  $[\alpha]_D^{25} - 33.3$  (c 0.1, CHCl<sub>3</sub>); (+)-HREIMS  $m/z$  304.2379 [M]<sup>+</sup> (calcd. for C<sub>20</sub>H<sub>32</sub>O<sub>2</sub>, 304.2397).

**Scalarin (7):** Yellow powder;  $[\alpha]_D^{25} + 41.2$  (c 0.1, CHCl<sub>3</sub>); (+)-HRESIMS  $m/z$  467.2767 [M + Na]<sup>+</sup> (calcd. for C<sub>27</sub>H<sub>40</sub>O<sub>5</sub>Na, 467.2773).

### 3.6. Cytotoxic Assays

Colorimetric MTT ((3-(4,5-Dimethylthiazol-2-yl)-2,5-diphenyltetrazolium bromide)) assays were carried out to assess the cell viability of the samples against a panel of five different cancer cell lines (i.e., human lung carcinoma A549 ATCC®CCL-185TM, human skin melanoma A2058 ATCC®CRL-11147TM, hepatocyte carcinoma HepG2 ATCC®HB-8065TM, breast adenocarcinoma MCF7 ATCC®HTB-22TM, and pancreas carcinoma MiaPaca-2 ATCC®CRL-1420TM). All cells were obtained from the American Type Culture Collection (ATCC, Manassas, VA, USA). A549 cells were grown in Ham's F12K medium with 2 mM glutamine, 10% fetal bovine serum (FBS), 100 U/mL penicillin, and 100  $\mu$ g/mL streptomycin. A2058 and HepG2 were grown in ATCC formulated Eagle's M essential medium (MEM) with 10% FBS, 2 mM l-glutamine, 1 mM sodium pyruvate, and 100  $\mu$ M MEM nonessential amino acids. MCF-7 cells were grown in the previous medium supplemented with 0.01 mg/mL of bovine insulin. MiaPaca-2 cells were grown in Dulbecco's modified Eagle's medium (DMEM) with 10% FBS, 100U/mL penicillin, and 100  $\mu$ g/mL streptomycin. The bioassays were performed as reported by Audoin et al. [20]. The cytotoxic activity was assessed after 72 h of treatment of the compound at the concentrations 0.098, 0.195, 0.391, 0.781, 1.563, 3.125, 6.250, 12.5, 25, 50, and 100  $\mu$ M.

## 4. Conclusions

In summary, two new spongian furanoditerpenes, **1** and **2**, together with five known terpenes, four furanoditerpenes **3–6** and one sesterterpene **7**, were isolated from sponge *Spongia tubulifera* collected in the Mexican Caribbean as its metabolic components. The absolute configurations of the new compounds **1** and **2** were determined by comparison of experimental and calculated ECD spectra.



Compounds **1**, **4**, and **6** displayed weak cytotoxic activity against a panel of five human tumor cell lines. This work represents the first chemical study of the secondary metabolites from *S. tubulifera*.

**Supplementary Materials:** The following are available online at <http://www.mdpi.com/1660-3397/17/7/416/s1>, Figures S1–S6: NMR spectra of **1** in CDCl<sub>3</sub>, Figure S7: HREIMS of **1**, Figures S7–S13: NMR spectra of **2** in CDCl<sub>3</sub>, Figure S14: (+)-HRESIMS of **2**, Figures S15–S23: NMR spectra of **3–7** in CDCl<sub>3</sub>, Table S1: NMR data of **1** in CDCl<sub>3</sub>, Table S2: NMR data of **2** in CDCl<sub>3</sub>.

**Author Contributions:** Conceptualization: C.J. and J.R.; Extraction process: D.P.-P. and C.A.S.-C.; Formal analysis: D.P.-P., J.R., and C.J.; Computational calculations: J.R., C.J., and D.P.-P.; Cytotoxic assays: B.C.; Investigation: D.P.-P.; Funding acquisition and Resources: J.R. and C.J.; Writing—original draft: D.P.-P.; Writing—review & editing: J.R. and C.J.

**Funding:** This work was supported by Grants AGL2015-63740-C2-2-R and RTC-2016-4611-1 (AEI/FEDER, EU) from the State Agency for Research (AEI) of Spain, both cofunded by the FEDER Programme from the European Union. DPP received a fellowship from the program National Council of Science and Technology (CONACYT) of Mexico and the Secretariat of Research, Innovation and Higher Education (SIIES) of Yucatan (Mexico).

**Acknowledgments:** We gratefully acknowledge the help of colleagues, Daniel Catzim Pech, Carlos González-Salas, Gabriel González Mapen, Jorge Peniche Pérez, Melissa Llanes López, and Rodrigo Garcia Uribe for collecting the marine samples. We thank Patricia Gomez for the taxonomic identification of the sponge. We would like to express our gratitude to Javier Sanchez-Cespedes for the antiviral assays and to Alejandro Beceiro for the antimicrobial evaluation.

**Conflicts of Interest:** The authors declare no conflict of interest.

## References

1. Máximo, P.; Ferreira, L.M.; Branco, P.; Lima, P.; Lourenço, A.; Benkendorff, K. The role of *Spongia* sp. In the discovery of marine lead compounds. *Mar. Drugs* **2016**, *14*, 139. [[CrossRef](#)] [[PubMed](#)]
2. Gonzalez, A.G.; Estrada, D.M.; Martin, J.D.; Martin, V.S.; Perez, C.; Perez, R. New antimicrobial diterpenes from the sponge *Spongia officinalis*. *Tetrahedron* **1984**, *40*, 4109–4113. [[CrossRef](#)]
3. Manzo, E.; Ciavatta, M.L.; Villani, G.; Varcamonti, M.; Sayem, S.M.A.; Van Soest, R.; Gavagnin, M. Bioactive terpenes from *Spongia officinalis*. *J. Nat. Prod.* **2011**, *74*, 1241–1247. [[CrossRef](#)] [[PubMed](#)]
4. Kohmoto, S.; Mcconnell, O.J.; Wright, A.; Cross, S. Isospongiadiol, a Cytotoxic and Antiviral Diterpene from a Caribbean Depp Water Marine Sponge, *Spongia* sp. *Chem. Lett.* **1987**, *16*, 1687–1690. [[CrossRef](#)]
5. Mori, D.; Kimura, Y.; Kitamura, S.; Sakagami, Y.; Yoshioka, Y.; Shintani, T.; Okamoto, T.; Ojika, M. Spongolactams, farnesyl transferase inhibitors from a marine sponge: Isolation through an LC/MS-guided assay, structures, and semisyntheses. *J. Org. Chem.* **2007**, *72*, 7190–7198. [[CrossRef](#)] [[PubMed](#)]
6. Phan, C.S.; Kamada, T.; Hamada, T.; Vairappan, C.S. Cytotoxic sesterterpenoids from bornean sponge *Spongia* sp. *Rec. Nat. Prod.* **2018**, *12*, 643–647. [[CrossRef](#)]
7. De Marino, S.; Iorizzi, M.; Zollo, F.; Debitus, C.; Menou, J.L.; Ospina, L.F.; Alcaraz, M.J.; Payá, M. New pyridinium alkaloids from a marine sponge of the genus *Spongia* with a human phospholipase A2 inhibitor profile. *J. Nat. Prod.* **2000**, *63*, 322–326. [[CrossRef](#)] [[PubMed](#)]
8. Anta, C.; González, N.; Santafé, G.; Rodríguez, J.; Jiménez, C. New xenia diterpenoids from the Indonesian soft coral *Xenia* sp. *J. Nat. Prod.* **2002**, *65*, 766–768. [[CrossRef](#)] [[PubMed](#)]
9. Urda, C.; Fernández, R.; Pérez, M.; Rodríguez, J.; Jiménez, C.; Cuevas, C. Protoxicins A and B, Cytotoxic Long-Chain Acylated Xenicanes from the Soft Coral *Protodendron repens*. *J. Nat. Prod.* **2017**, *80*, 713–719. [[CrossRef](#)] [[PubMed](#)]
10. Tarazona, G.; Bénédict, G.; Fernández, R.; Pérez, M.; Rodríguez, J.; Jiménez, C.; Cuevas, C. Can Stereoclusters Separated by Two Methylene Groups Be Related by DFT Studies? the Case of the Cytotoxic Meroditerpenes Halioxepines. *J. Nat. Prod.* **2018**, *81*, 343–348. [[CrossRef](#)]
11. Carballeira, N.M.; Shalabi, F.; Cruz, C.; Rodriguez, J.; Rodriguez, E. Comparative study of the fatty acid composition of sponges of the genus *Ircinia*. Identification of the new 23-methyl-5,9-tetracosadienoic acid. *Comp. Biochem. Physiol.* **1991**, *100*, 489–492. [[CrossRef](#)]
12. Galeano, E.; Martínez, A. Antimicrobial activity of marine sponges from Urabá Gulf, Colombian Caribbean region. *J. Mycol. Med.* **2007**, *17*, 21–24. [[CrossRef](#)]
13. Searle, P.A.; Molinski, T.F. Scalemic 12-hydroxyambliofuran and 12-acetoxy-ambliofuran, five tetracyclic furanoditerpenes and a furanosesterterpene from *Spongia* sp. *Tetrahedron* **1994**, *50*, 9893–9908. [[CrossRef](#)]

14. Yong, K.W.L.; Mudianta, I.W.; Cheney, K.L.; Mollo, E.; Blanchfield, J.T.; Garson, M.J. Isolation of norsesiterterpenes and spongian diterpenes from *Dorisprismatica* (= *Glossodoris*) *atromarginata*. *J. Nat. Prod.* **2015**, *78*, 421–430. [[CrossRef](#)] [[PubMed](#)]
15. Gunasekera, S.P.; Schmitz, F.J. New Spongian Diterpenoids from a Great Barrier Reef Sponge, *Spongia* sp. *J. Org. Chem.* **1991**, *56*, 1250–1253. [[CrossRef](#)]
16. Kazlauskas, R.; Murphy, P.T.; Wells, R.J.; Noack, K.; Oberhänsli, W.E.; Schönholzer, P. A New Series of Diterpenes from Australian *Spongia* Species. *Aust. J. Chem.* **1979**, *32*, 867–880. [[CrossRef](#)]
17. Walker, R.P.; Rosser, R.M.; Faulkner, J. Two New Metabolites of the Sponge *Dysidea amblia* and Revision of the Structure of Ambliol C. *J. Org. Chem.* **1984**, *49*, 5160–5163. [[CrossRef](#)]
18. Fattorusso, E.; Magno, S.; Santacroce, C.; Sica, D. Scalarin, a New Pentacyclic C-25 Terpenoid from the Sponge *Cacospongia scalaris*. *Tetrahedron* **1972**, *28*, 5993–5997. [[CrossRef](#)]
19. Cimino, B.G.; De Stefano, S.; Minale, L.; Trivellone, E. 12-epi-Scalarin and 12-epi-Deoxoscalarin, Sesterterpenes from the Sponge *Spongia Nitens*. *J. Chem. Soc. Perkin I.* **1977**, *1*, 1587–1593. [[CrossRef](#)]
20. Audoin, C.; Bonhomme, D.; Ivanisevic, J.; De La Cruz, M.; Cautain, B.; Monteiro, M.C.; Reyes, F.; Rios, L.; Perez, T.; Thomas, O.P. Balibalosides, an original family of glucosylated sesterterpenes produced by the Mediterranean sponge *Oscarella balibaloi*. *Mar. Drugs* **2013**, *11*, 1477–1489. [[CrossRef](#)]
21. Longley, R.E.; McConnell, O.J.; Essich, E.; Harmody, D. Evaluation of marine sponge metabolites for cytotoxicity and signal transduction activity. *J. Nat. Prod.* **1993**, *56*, 915–920. [[CrossRef](#)] [[PubMed](#)]
22. Thompson, J.E.; Walker, R.P.; Faulkner, D.J. Screening and bioassays for biologically-active substances from forty marine sponge species from San Diego, California, USA. *Mar. Biol.* **1985**, *88*, 11–21. [[CrossRef](#)]
23. Bruhn, T.; Schaumlöffel, A.; Hemberger, Y.; Bringmann, G. SpecDis: Quantifying the Comparison of Calculated and Experimental Electronic Circular Dichroism Spectra. *Chirality* **2013**, *25*, 243–249. [[CrossRef](#)] [[PubMed](#)]



© 2019 by the authors. Licensee MDPI, Basel, Switzerland. This article is an open access article distributed under the terms and conditions of the Creative Commons Attribution (CC BY) license (<http://creativecommons.org/licenses/by/4.0/>).